Acta Cryst. (1973). B29, 2046

$Ca_4(PO_4)_2O$, Tetracalcium Diphosphate Monoxide. Crystal Structure and Relationships to $Ca_5(PO_4)_3OH$ and $K_3Na(SO_4)_2$

By B. Dickens, W. E. Brown,* G. J. Kruger† and J. M. Stewart‡

Dental Research Section, National Bureau of Standards, Washington, D. C. 20234, *U.S.A.*

(*Received* 17 *January* 1973; *accepted* 27 *April* 1973)

$Ca_4(PO_4)_2O$, tetracalcium diphosphate monoxide, crystallizes in the monoclinic unit cell $a = 7{\cdot}023$ (1), $b = 11{\cdot}986$ (4), $c = 9{\cdot}473$ (2) Å, $\beta = 90{\cdot}90$ (1)° (at 25 °C) in space group $P2_1$ with 4[$Ca_4(PO_4)_2O$] per cell. 3288 X-ray data were measured from a single crystal by θ–2θ scans using Mo $K\alpha$ radiation; 56 of these reflections were of 'unobservable' intensity. The structure was solved by an application of direct phasing methods and subsequent calculation of an E map. It was refined anisotropically by full-matrix least squares to $R_w(F) = 0{\cdot}036$, $R(F) = 0{\cdot}037$. Allowance was made for isotropic secondary extinction but not for anomalous scattering or absorption. The dimensions of the unit cells of $Ca_4(PO_4)_2O$ and $Ca_5(PO_4)_3OH$ (hydroxyapatite), an idealized form of the major inorganic phase in the human body, are simply related. Although this 3-dimensional relationship in the unit-cell shapes is not carried over into the details of the actual structures, $Ca_4(PO_4)_2O$ does contain a layer which is similar to a layer in $Ca_5(PO_4)_3OH$, and an epitaxic relationship between the two compounds is conceivable. $Ca_4(PO_4)_2O$ is also related to the $K_3Na(SO_4)_2$ (glaserite) structure. In this relationship the oxide ions are 'extra' ions. One Ca ion in $Ca_4(PO_4)_2O$ is weakly coordinated to a face of a PO_4 group, a feature which has been previously observed for Ca only in a disordered cation site in β-$Ca_3(PO_4)_2$. The two crystallographically discrete oxide ions are surrounded by tetrahedra of Ca ions, with Ca···O distances in the range 2·136 (4) to 2·277 (3) Å. Thus, the oxide ions do not lie in a channel formed by cations in the structure and $Ca_4(PO_4)_2O$ cannot be considered to be an oxyapatite. The positions of the P atoms and the Ca and oxide ions lie close to those required by space group *Pmcn*. This explains the appreciable twinning exhibited by $Ca_4(PO_4)_2O$. It also makes the existence of a higher-symmetry modification feasible.

Introduction

This investigation is the sequel to an earlier investigation (Brown & Epstein, 1965) on $Ca_4(PO_4)_2O$, tetracalcium diphosphate monoxide. The more usual name for $Ca_4(PO_4)_2O$ is tetracalcium phosphate, from the formula when written as $4CaO.P_2O_5$. Brown & Epstein showed that $Ca_4(PO_4)_2O$ may have a structural relationship to $Ca_5(PO_4)_3(OH,F)$ (Kay, Young & Posner, 1964), the mineral hydroxyapatite, which may be considered an idealized form of the major inorganic phase in the human body. Here we report on the determination of the crystal structure of $Ca_4(PO_4)_2O$ using a small single crystal, and discuss the $Ca_4(PO_4)_2O$–$Ca_5(PO_4)_3OH$ and $Ca_4(PO_4)_2O$–$K_3Na(SO_4)_2$ relationships.

Data collection and structure refinement

The crystal used in the data collection was an irregular colorless disc with radius ~0·33 mm, thickness ~0·11 mm. This was the largest untwinned crystal found in the sample described by Brown & Epstein (1965). The crystal was attached to the goniometer head in our usual way (Dickens & Bowen, 1971). Crystal data are as follows.

Formula (ideal): $Ca_4(PO_4)_2O$.
Cell at 25 °C: monoclinic
$a = 7{\cdot}023$ (1) Å
$b = 11{\cdot}986$ (4)
$c = 9{\cdot}473$ (2)
$\beta = 90{\cdot}90$ (1)°.
Volume = 797·3 $Å^3$.
Space group $P2_1$; cell contents 4[$Ca_4(PO_4)_2O$].
Calculated density 3·051 g cm^{-3}.
Observed density 3·06 g cm^{-3} (Bücking & Linck, 1887).

The cell parameters and their standard deviations (given in parentheses) were calculated by least-squares methods from 20 2θ values observed on a diffractometer using Mo $K\alpha$ radiation filtered through 0·025 mm Nb foil. The wavelength $\lambda(\text{Mo } K\alpha) = 0{\cdot}710688$ Å was assumed. (To make b the unique monoclinic axis, the cell a',b',c' given by Brown and Epstein has been transformed here to c,a,b.)

The X-ray data were measured using the θ–2θ procedure described by Alexander & Smith (1962; 1964) and as adapted by Reimann, Mighell & Mauer (1967). Each reflection was measured only once. There were 3288 independent reflections of which 56 were 'unobserved' [*i.e.* $I_{hkl} < 2\sigma(I_{hkl})$]. μ(Mo) was taken to be

---

* Director, American Dental Association Research Unit at the National Bureau of Standards.

† Postdoctoral fellow, Department of Computer Science, University of Maryland, 1970–1971. Permanent address: National Physical Research Laboratory, South African Council for Scientific and Industrial Research, Pretoria, Republic of South Africa.

‡ Department of Chemistry, University of Maryland, College Park, Maryland 20742, U.S.A.

30·3 cm^{-1}. Because of the small crystal size, absorption corrections were neglected; the resultant maximum error in F_o is estimated to be 5% for the 2θ range 0 to 80°.

The structure was determined using the sequence *DATRDN-NORMSF-SINGEN-APHASE-TANGEN-FOURR* in the X-ray system of Stewart, Kruger, Ammon, Dickinson & Hall (1972). The quasi-normalized structure-factor statistics (Dickinson, Stewart & Holden, 1966) were very close (see below) to those expected for an acentric space group. In the following list, E is the quasi-normalized structure factor and the values in square brackets are the theoretical values for an acentric structure. Quantities enclosed in $\langle\ \rangle$ brackets are average values. $\langle|E|\rangle=0{\cdot}886$ [0·886], $\langle|E^2-1|\rangle=0{\cdot}748$ [0·736], $\langle|E^2-1|^2\rangle=1{\cdot}061$ [1·000], $\langle|E^2-1|^3\rangle=3{\cdot}186$ [2·000]; $\%E>3{\cdot}0=0{\cdot}05$ [0·01], $\%E>2{\cdot}5=0{\cdot}22$ [0·19], $\%E>2{\cdot}0=1{\cdot}95$ [1·83], $\%E>1{\cdot}8=4{\cdot}10$ [3·92], $\%E>1{\cdot}6=7{\cdot}91$ [7·73], $\%E>1{\cdot}4=14{\cdot}6$ [14·1], $\%E>1{\cdot}2=23{\cdot}9$ [23·7], $\%E>1{\cdot}0=35{\cdot}9$ [36·8].

The following phases were fixed during the tangent refinement part of the program: [1] 400 (0); [6] 440 (90); [24] 013 (0); [29] 1,0,$\overline{13}$ (0); [89] 803 (0), where the values given are [sequence number in ordered list of E values] hkl (phase in °). The tangent refinement was carried out in four stages, using 100, 150, 225 and then 300 E values (minimum E's were 1·981, 1·887, 1·661 and 1·563, respectively). The 300 E values from the final cycle were used to calculate an E map which contained peaks at the Ca and P positions as its salient features. The oxygen atoms were found in a subsequent F_o Fourier synthesis phased from the Ca and P atoms.

The structure was refined isotropically using the X-RAY System program *CRYLSQ* to $R_w=0{\cdot}041$, $R=0{\cdot}050$, and then anisotropically in a series of block refinements (varying half of the structure at any one time) to $R_w=0{\cdot}036$, $R=0{\cdot}037$. The y coordinate of Ca(1) was fixed to define the origin along [010]. The scattering factors used were those for the neutral atoms in *International Tables for X-ray Crystallography* (1962). Before the anisotropic refinements, the weighting scheme was changed from one based on counting statistics, $\sigma_c(F)$, to $w(F)=[\sigma_c^2(F)+0{\cdot}0005\ F_o^2]^{-1}$. In the final refinement the average shift/error was 0·005 and the standard deviation of an observation of unit weight was 0·34. The extinction parameter g (Zachariasen, 1963, 1967; Larson, 1970) refined to 1·38 (6) $(\times 10^{-4})^{\circ}$ (for an isotropic Gaussian distribution of mosaic blocks). The largest correlation coefficients are 0·64 between the extinction and scale factors, and 0·50 to 0·59 between the y parameters of the pairs of atoms [Ca(4), Ca(5)], [Ca(5), Ca(6)], [Ca(5), Ca(8)], and [Ca(6), Ca(8)]. The three largest peaks and two largest 'holes' in a difference electron density synthesis calculated after the final refinement were $\sim 0{\cdot}8$ e Å^{-3} and $\sim -0{\cdot}8$ e Å^{-3}, respectively. They are all attributed to the background.

The atomic parameters are given in Table 1 and the observed and calculated structure factors in Table 2.

Table 1. *Atomic parameters of* $Ca_4(PO_4)_2O$

Thermal parameters have the form $\exp[-2\pi^2(U_{11}h^2a^{*2}+U_{22}k^2b^{*2}+U_{33}l^2c^{*2}+2U_{12}hka^*b^*+2U_{13}hla^*c^*+2U_{23}klb^*c^*)]$.

Figures in parentheses are standard deviations in last significant digit.

	x	y	z	10^2U_{11}*	10^2U_{22}	10^2U_{33}	10^2U_{12}	10^2U_{13}	10^2U_{23}
Ca(1)	0·0311 (1)	0·3444	0·89441 (9)	0·59 (4)	0·59 (4)	0·82 (4)	0·01 (3)	−0·12 (3)	0·03 (3)
Ca(2)	0·5320 (1)	0·3000 (1)	0·89733 (9)	0·66 (4)	0·82 (4)	0·77 (4)	−0·14 (4)	−0·08 (3)	−0·02 (4)
Ca(3)	0·7654 (1)	0·3040 (1)	0·5299 (1)	2·07 (5)	0·45 (5)	1·29 (4)	0·00 (4)	−0·20 (4)	−0·07 (4)
Ca(4)	0·2685 (1)	0·3000 (1)	0·25229 (9)	0·70 (4)	0·54 (4)	0·64 (3)	0·05 (4)	−0·06 (3)	−0·04 (4)
Ca(5)	0·7409 (1)	0·1068 (1)	0·25600 (9)	0·66 (4)	0·81 (5)	0·71 (4)	−0·04 (4)	−0·11 (3)	0·00 (3)
Ca(6)	0·2501 (1)	0·0798 (1)	0·01201 (9)	0·96 (4)	0·58 (4)	0·70 (4)	−0·08 (3)	0·02 (3)	−0·06 (3)
Ca(7)	−0·0099 (1)	0·0700 (1)	0·63310 (9)	0·72 (4)	1·01 (5)	0·89 (4)	0·27 (4)	−0·07 (3)	0·23 (4)
Ca(8)	0·5146 (1)	0·0520 (1)	0·59216 (9)	0·60 (4)	0·71 (5)	1·09 (4)	−0·04 (3)	−0·04 (3)	−0·17 (3)
P(1)	0·7665 (2)	0·3921 (1)	0·2140 (1)	0·64 (5)	0·57 (6)	0·57 (5)	−0·02 (4)	−0·07 (4)	−0·02 (4)
P(2)	0·2893 (2)	0·3247 (1)	0·6240 (1)	0·80 (5)	0·55 (6)	0·61 (5)	−0·06 (4)	0·00 (4)	0·00 (4)
P(3)	0·2376 (2)	0·0400 (1)	0·3181 (1)	0·59 (5)	0·59 (6)	0·51 (4)	−0·04 (4)	−0·08 (4)	0·00 (4)
P(4)	0·7641 (2)	0·0773 (1)	0·9104 (1)	0·54 (5)	0·56 (6)	0·62 (4)	−0·04 (4)	−0·10 (4)	−0·07 (4)
O(11)	0·7319 (5)	0·5180 (3)	0·2667 (3)	1·2 (2)	0·5 (2)	0·8 (1)	0·3 (1)	−0·3 (1)	−0·1 (1)
O(12)	0·6113 (4)	0·3244 (3)	0·2860 (3)	1·0 (1)	2·2 (2)	1·3 (1)	−0·6 (1)	−0·1 (1)	0·9 (1)
O(13)	0·9541 (5)	0·3663 (3)	0·2936 (3)	1·1 (2)	1·2 (2)	1·5 (2)	0·2 (1)	−0·5 (1)	−0·3 (1)
O(14)	0·7702 (5)	0·3650 (3)	0·0556 (3)	1·6 (2)	1·6 (2)	0·6 (1)	−0·5 (1)	0·0 (1)	−0·2 (1)
O(21)	0·2867 (5)	0·4090 (3)	0·7480 (3)	1·3 (2)	0·9 (2)	0·8 (1)	0·1 (1)	0·1 (1)	−0·1 (1)
O(22)	0·0960 (5)	0·2645 (3)	0·6226 (3)	1·0 (2)	1·1 (2)	2·4 (2)	−0·1 (1)	−0·5 (1)	−0·1 (1)
O(23)	0·4557 (5)	0·2434 (3)	0·6594 (3)	1·2 (2)	1·0 (2)	1·5 (2)	0·5 (1)	−0·1 (1)	−0·4 (1)
O(24)	0·3309 (6)	0·3802 (3)	0·4843 (3)	4·1 (2)	1·1 (2)	0·6 (1)	−0·8 (2)	0·7 (2)	−0·2 (1)
O(31)	0·2165 (5)	0·0041 (3)	0·4737 (3)	1·7 (2)	1·0 (2)	0·7 (1)	0·3 (1)	0·0 (1)	0·2 (1)
O(32)	0·0766 (5)	0·1137 (3)	0·2636 (3)	1·7 (2)	1·0 (2)	0·7 (1)	0·3 (1)	0·0 (1)	0·2 (1)
O(33)	0·4194 (5)	0·1082 (3)	0·3023 (4)	0·9 (2)	0·9 (2)	3·5 (2)	0·0 (1)	0·2 (1)	0·4 (2)
O(34)	0·2444 (5)	−0·0682 (3)	0·2282 (3)	1·4 (2)	1·6 (2)	1·3 (2)	0·5 (1)	−0·1 (1)	−0·8 (1)
O(41)	0·5890 (5)	0·1053 (3)	0·9992 (3)	1·0 (1)	1·7 (2)	1·0 (1)	0·1 (1)	0·1 (1)	−0·5 (1)
O(42)	0·8384 (5)	0·1855 (3)	0·8407 (3)	2·0 (2)	0·3 (2)	1·4 (2)	−0·2 (1)	−0·1 (1)	0·1 (1)
O(43)	0·7164 (5)	−0·0028 (3)	0·7862 (3)	1·5 (2)	0·6 (2)	0·8 (1)	0·1 (1)	−0·3 (1)	−0·3 (1)
O(44)	0·9190 (5)	0·0290 (3)	1·0085 (3)	1·2 (2)	1·3 (2)	1·4 (2)	0·0 (1)	−0·8 (1)	0·1 (1)
O(1)	0·2642 (5)	0·2629 (3)	0·0163 (3)	1·0 (1)	0·7 (2)	0·8 (1)	0·0 (1)	0·0 (1)	−0·1 (1)
O(2)	0·7656 (5)	0·1282 (3)	0·4905 (3)	1·1 (2)	0·6 (2)	0·6 (1)	0·1 (1)	−0·2 (1)	−0·1 (1)

Description of the structure

The structure of $Ca_4(PO_4)_2O$ is shown in Fig. 1. There are eight unique Ca ions, four PO_4 groups and two oxide ions. The Ca and P atoms lie near four sheets perpendicular to [010], two adjacent sheets being crystallographically related to the other two in the cell by the twofold screw axis of the space group, $P2_1$. Each sheet contains two cation–anion columns and one cation–cation column. These columns are [Ca(1),

Table 2. *Calculated and observed structure factors for* $Ca_4(PO_4)_2O$

Columns are l, $10F_o$, $10F_c$ and $10\,\sigma(F_o)$.

Unobserved reflections are those with intensity less than $2\sigma(I)$ and are marked by *.

Table 2 (*cont.*)

Ca(2)], [Ca(3), P(2)O_4] and [Ca(4), P(1)O_4] in one sheet (Fig. 2) and [Ca(7), Ca(8)], [Ca(5), P(3)O_4] and [Ca(6), P(4)O_4] in the other (Fig. 3).

The calcium ion environments

Ca(1) is coordinated to seven oxygen atoms (see Fig. 2), including the PO_4 edge [O(21), O(22)] and the oxide ion O(1), arranged in an approximately pentagonal bipyramid (see Table 3 for details of all ionic environments).

Ca(2) is coordinated to seven oxygen atoms, including the PO_4 edges [O(21), O(23)] and [O(41), O(42)], and the oxide ion O(1). The coordination polyhedron of Ca(2) is irregular.

Ca(3) is coordinated to seven oxygen atoms, including the PO_4 edges [O(12), O(13)] and [O(31), O(34)], and to the oxide ion O(2). Six of the oxygens in the coordination of Ca(3) may be considered to be arranged in a partial pentagonal bipyramid. The seventh member of the coordination polyhedron is O(34), which is necessarily displaced from the remaining equatorial position of the pentagonal bipyramid because it is the second member of the [O(31), O(34)] PO_4 edge. It is the oxygen with the weakest bond to Ca(3).

Ca(4) is coordinated to seven oxygen atoms, including the PO_4 edge [O(32), O(33)], and the O(1) oxide ion. The coordination geometry of Ca(4) is derived from pentagonal bipyramidal, with O(1) occupying one of the axial positions.

Ca(5) is coordinated to seven oxygen atoms (Fig. 3), including the PO_4 edges [O(41), O(44)] and [O(12), O(13)], and the oxide ion O(2). The coordination of Ca(5) is derived from pentagonal bipyramidal with [O(41), O(44)] in the equator.

Ca(6) is coordinated to eight oxygen atoms, including the PO_4 edge [O(11), O(14)], and the oxide ion O(1). The coordination polyhedron of Ca(6) may be considered to include the PO_4 face [O(32), O(33), O(34)],

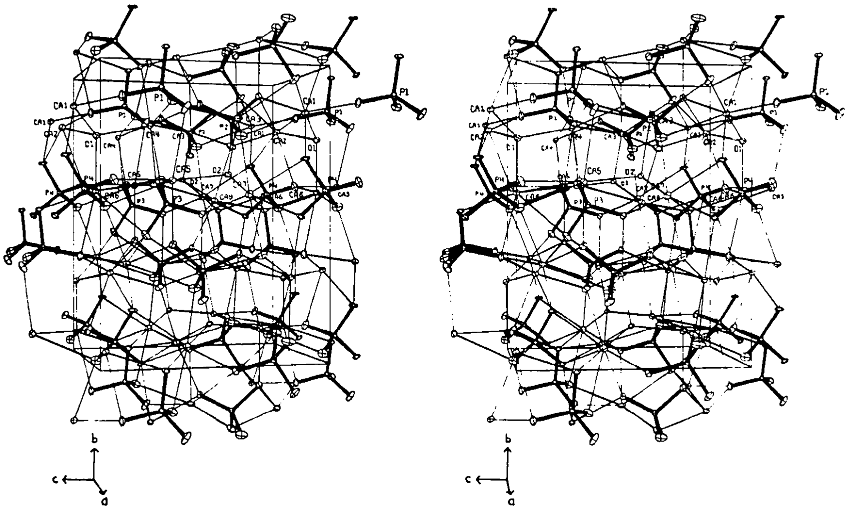

Fig. 1. A stereoscopic view of the $Ca_4(PO_4)_2O$ structure viewed along [100]. The origin of the crystallographic coordinate system is at the lower right front corner of the unit cell. Only a unique set of atoms is labelled.

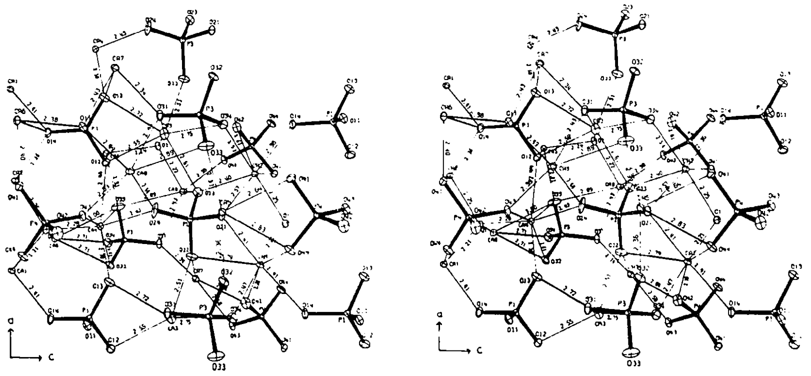

Fig. 2. The environments of the Ca(1), Ca(2), Ca(3), Ca(4), $P(1)O_4$ and $P(2)O_4$ ions in $Ca_4(PO_4)_2O$. These ions lie in the same sheet parallel to (010).

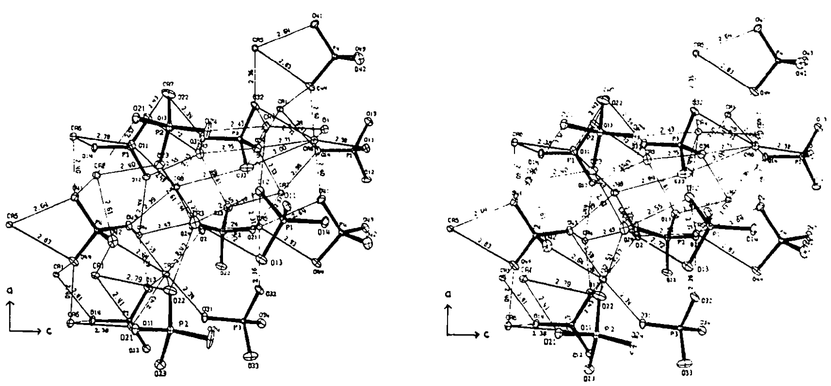

Fig. 3. The environments of the Ca(5), Ca(6), Ca(7), Ca(8), $P(3)O_4$ and $P(4)O_4$ ions in $Ca_4(PO_4)_2O$. These ions lie in the same sheet parallel to (010).

although the primary ionic bonding of all these three oxygen atoms is to neighboring Ca ions. Coordination of Ca to a PO_4 face is rare; the other known example is in the β-$Ca_3(PO_4)_2$ structure (Dickens, Bowen & Brown, 1971).

Ca(7) is coordinated to seven oxygen atoms, including the PO_4 edges [O(11), O(13)] and [O(42), O(43)], and the oxide ion O(2). The coordination geometry is irregular.

Ca(8) is coordinated to seven oxygen atoms, including the PO_4 edge [O(31), O(33)], and the oxide ion O(2). The coordination is pentagonal bipyramidal with the above oxygens in equatorial positions, along with O(11) and O(43).

Proceeding on the assumption that any Ca···O distance less than ~2·5 Å denotes a strong Ca···O bond, we note that the bonding of all Ca ions to the oxide ions O(1) and O(2) is strong. The numbers of strong and less strong bonds respectively to all coordinated oxygens from individual Ca ions are as follows:

Ca(1) 6:1; Ca(2) 3:4; Ca(3) 2:5; Ca(4) 5:2; Ca(5) 4:3; Ca(6) 4:4; Ca(7) 4:3; Ca(8) 6:2.

The PO_4 *environments*

In the $P(1)O_4$ group (Fig. 2), each oxygen is bonded to three Ca ions. The $P(1)O_4$ edges [O(11), O(13)], [O(11), O(14)] and [O(12), O(13)] are 'shared' by coordination to Ca ions.

Table 3. *Distances and angles in the* $Ca_4(PO_4)_2O$ *structure*

The figures in parentheses are the standard deviations in the last significant digit.

Cation environments	
Ca(1)–O(1)	2·214 (3) Å
Ca(1)–O(42)	2·384 (3)
Ca(1)–O(21)	2·412 (3)
Ca(1)–O(14)	2·415 (3)
Ca(1)–O(44)	2·416 (4)
Ca(1)–O(34)	2·474 (4)
Ca(1)–O(22)	2·788 (4)
Ca(2)–O(1)	2·251 (3)
Ca(2)–O(14)	2·360 (3)
Ca(2)–O(23)	2·403 (3)
Ca(2)–O(34)	2·534 (4)
Ca(2)–O(41)	2·550 (4)
Ca(2)–O(21)	2·567 (3)
Ca(2)–O(42)	2·613 (4)
Ca(3)–O(2)	2·136 (4)
Ca(3)–O(31)	2·399 (4)
Ca(3)–O(22)	2·515 (4)
Ca(3)–O(12)	2·546 (3)
Ca(3)–O(23)	2·615 (4)
Ca(3)–O(13)	2·721 (3)
Ca(3)–O(34)	2·755 (4)
Ca(4)–O(1)	2·277 (3)
Ca(4)–O(13)	2·383 (4)
Ca(4)–O(43)	2·389 (4)
Ca(4)–O(24)	2·429 (3)
Ca(4)–O(12)	2·441 (3)
Ca(4)–O(33)	2·570 (4)
Ca(4)–O(32)	2·608 (4)
Ca(5)–O(2)	2·238 (3)
Ca(5)–O(33)	2·307 (4)
Ca(5)–O(32)	2·359 (3)
Ca(5)–O(21)	2·376 (4)
Ca(5)–O(41)	2·639 (3)
Ca(5)–O(12)	2·774 (4)
Ca(5)–O(44)	2·829 (3)
Ca(6)–O(1)	2·193 (4)
Ca(6)–O(11)	2·381 (3)
Ca(6)–O(44)	2·404 (3)
Ca(6)–O(41)	2·404 (3)
Ca(6)–O(14)	2·652 (4)
Ca(6)–O(34)	2·706 (4)
Ca(6)–O(32)	2·713 (3)
Ca(6)–O(33)	2·996 (4)
Ca(7)–O(2)	2·174 (3)
Ca(7)–O(31)	2·345 (3)
Ca(7)–O(11)	2·425 (3)
Ca(7)–O(22)	2·446 (4)
Ca(7)–O(13)	2·563 (4)
Ca(7)–O(43)	2·576 (3)
Ca(7)–O(42)	2·369 (4)
Ca(8)–O(2)	2·217 (3) Å
Ca(8)–O(43)	2·394 (3)
Ca(8)–O(23)	2·414 (4)
Ca(8)–O(31)	2·428 (3)
Ca(8)–O(24)	2·440 (4)
Ca(8)–O(11)	2·488 (3)
Ca(8)–O(33)	2·892 (4)
Ca(8)–O(12)	3·092 (4)
PO_4 groups	
P(1)—O(11)	1·531 (4)
P(1)—O(12)	1·527 (4)
P(1)—O(13)	1·539 (4)
P(1)—O(14)	1·534 (3)
O(11)–O(12)	2·533 (5)
O(11)–O(13)	2·471 (5)
O(11)–O(14)	2·461 (5)
O(12)–O(13)	2·459 (5)
O(12)–O(14)	2·512 (5)
O(13)–O(14)	2·579 (5)
O(11)–P(1)–O(12)	111·8 (2)°
O(11)–P(1)–O(13)	107·2 (2)
O(11)–P(1)–O(14)	106·8 (2)
O(12)–P(1)–O(13)	106·6 (2)
O(12)–P(1)–O(14)	110·3 (2)
O(13)–P(1)–O(14)	114·1 (2)
P(2)—O(21)	1·547 (4) Å
P(2)—O(22)	1·537 (4)
P(2)—O(23)	1·553 (4)
P(2)—O(24)	1·511 (4)
O(21)–O(22)	2·478 (5)
O(21)–O(23)	2·462 (5)
O(21)–O(24)	2·542 (4)
O(22)–O(23)	2·557 (5)
O(22)–O(24)	2·533 (5)
O(23)–O(24)	2·479 (5)
O(21)–P(2)–O(22)	107·0 (2)°
O(21)–P(2)–O(23)	105·2 (2)
O(21)–P(2)–O(24)	112·5 (2)
O(22)–P(2)–O(23)	111·7 (2)
O(22)–P(2)–O(24)	112·4 (2)
O(23)–P(2)–O(24)	108·0 (2)
P(3)—O(31)	1·543 (3) Å
P(3)—O(32)	1·521 (4)
P(3)—O(33)	1·524 (4)
P(3)—O(34)	1·550 (4)
O(31)–O(32)	2·572 (5)
O(31)–O(33)	2·506 (5)
O(31)–O(34)	2·489 (5)
O(32)–O(33)	2·431 (5)
O(32)–O(34)	2·498 (5)
O(33)–O(34)	2·535 (5)
O(31)–P(3)–O(32)	114·1 (2)°
O(31)–P(3)–O(33)	109·6 (2)
O(31)–P(3)–O(34)	107·2 (2)
O(32)–P(3)–O(33)	106·0 (2)
O(32)–P(3)–O(34)	108·9 (2)
O(33)–P(3)–O(34)	111·1 (2)
P(4)—O(41)	1·537 (3) Å
P(4)—O(42)	1·547 (4)
P(4)—O(43)	1·549 (3)
P(4)—O(44)	1·532 (4)
O(41)–O(42)	2·513 (5)
O(41)–O(43)	2·567 (5)
O(41)–O(44)	2·491 (5)
O(42)–O(43)	2·462 (5)
O(42)–O(44)	2·515 (5)
O(43)–O(44)	2·550 (5)
O(41)–P(4)–O(42)	109·1 (2)°
O(41)–P(4)–O(43)	112·6 (2)
O(41)–P(4)–O(44)	108·5 (2)
O(42)–P(4)–O(43)	105·3 (2)
O(42)–P(4)–O(44)	109·5 (2)
O(43)–P(4)–O(44)	111·7 (2)
Oxygen atom environments	
(i) oxide ions	
O(1)–Ca(6)	2·173 (4) Å
O(1)–Ca(1)	2·214 (3)
O(1)–Ca(2)	2·251 (3)
O(1)–Ca(4)	2·277 (3)
O(2)–Ca(3)	2·136 (4)
O(2)–Ca(7)	2·174 (3)
O(2)–Ca(8)	2·217 (3)
O(2)–Ca(5)	2·238 (3)
Ca(6)–O(1)–Ca(1)	113·4 (1)°
Ca(6)–O(1)–Ca(2)	103·0 (1)
Ca(6)–O(1)–Ca(4)	102·3 (1)
Ca(1)–O(1)–Ca(2)	105·6 (1)
Ca(1)–O(1)–Ca(4)	115·1 (1)
Ca(2)–O(1)–Ca(4)	117·0 (1)
Ca(3)–O(2)–Ca(7)	102·1 (1)
Ca(3)–O(2)–Ca(8)	109·0 (1)
Ca(3)–O(2)–Ca(5)	106·6 (1)
Ca(7)–O(2)–Ca(8)	100·0 (1)
Ca(7)–O(2)–Ca(5)	128·6 (2)
Ca(8)–O(2)–Ca(5)	109·5 (1)
(ii) PO_4 oxygens	
O(11)–Ca(6)	2·381 (3) Å
O(11)–Ca(7)	2·425 (3)
O(11)–Ca(8)	2·488 (3)
O(12)–Ca(4)	2·441 (3)
O(12)–Ca(3)	2·546 (3)
O(12)–Ca(5)	2·774 (4)
O(13)–Ca(4)	2·383 (4) Å
O(13)–Ca(7)	2·563 (4)
O(13)–Ca(3)	2·721 (3)
O(14)–Ca(2)	2·360 (3)
O(14)–Ca(1)	2·415 (3)
O(14)–Ca(6)	2·652 (4)
O(21)–Ca(5)	2·376 (4)
O(21)–Ca(1)	2·412 (3)
O(21)–Ca(2)	2·567 (3)
O(22)–Ca(7)	2·446 (4)
O(22)–Ca(3)	2·515 (4)
O(22)–Ca(1)	2·788 (4)
O(23)–Ca(2)	2·403 (3)
O(23)–Ca(8)	2·414 (4)
O(23)–Ca(3)	2·615 (4)
O(24)–Ca(4)	2·429 (3)
O(24)–Ca(8)	2·440 (4)
O(31)–Ca(7)	2·345 (3)
O(31)–Ca(3)	2·399 (4)
O(31)–Ca(8)	2·428 (3)
O(32)–Ca(5)	2·359 (3)
O(32)–Ca(4)	2·608 (4)
O(32)–Ca(6)	2·713 (3)
O(33)–Ca(5)	2·307 (4)
O(33)–Ca(4)	2·570 (4)
O(33)–Ca(8)	2·892 (4)
O(33)–Ca(6)	2·996 (4)
O(34)–Ca(1)	2·474 (4)
O(34)–Ca(2)	2·534 (4)
O(34)–Ca(6)	2·706 (4)
O(34)–Ca(3)	2·755 (4)
O(41)–Ca(6)	2·404 (3)
O(41)–Ca(2)	2·550 (4)
O(41)–Ca(5)	2·639 (3)
O(42)–Ca(1)	2·384 (3)
O(42)–Ca(2)	2·613 (4)
O(42)–Ca(7)	2·639 (4)
O(43)–Ca(4)	2·389 (4)
O(43)–Ca(8)	2·394 (3)
O(43)–Ca(7)	2·576 (3)
O(44)–Ca(6)	2·404 (3)
O(44)–Ca(1)	2·416 (4)
O(44)–Ca(5)	2·829 (3)

In the $P(2)O_4$ group, O(21), O(22) and O(23) are each coordinated to three Ca ions, and O(24) is coordinated to two. The edges [O(21), O(22)] and [O(21), O(23)] are 'shared'.

In the $P(3)O_4$ group (Fig. 3), O(31) and O(32) are both bonded to three Ca ions, while O(33) and O(34) may be considered to be bonded to four. The edges [O(31), O(33)], [O(31), O(34)] and [O(32), O(33)] are 'shared', as is the [O(32), O(33), O(34)] face. As judged from the O···Ca distances for the $P(3)O_4$ group, the bonding of the $P(3)O_4$ oxygens to Ca(8) and Ca(6) is weak, apparently because of repulsion of these Ca ions by the other two Ca ions, Ca(5) and Ca(4), to which the $P(3)O_4$ oxygens are bonded more strongly.

In the $P(4)O_4$ group, each oxygen is bonded to three Ca ions and the edges [O(41), O(42)], [O(41), O(44)] and [O(42), O(43)] are 'shared'.

In all PO_4 groups, the O–P–O angles less than the tetrahedral angle, 109·5°, are associated with PO_4 edges which are coordinated to Ca, in accord with Pauling's (1960, p. 559) rule.

The oxide ion environments

Oxide ion O(1) is coordinated very strongly to the Ca(1), Ca(2), Ca(4) and Ca(6) ions, which are arranged in an approximate tetrahedron about O(1). Ca(6) is in a different sheet from the other Ca ions. Oxide ion O(2) is similarly coordinated to Ca(5), Ca(7), Ca(8) in one sheet and Ca(3) in another. The O(1)···Ca and O(2)···Ca distances (Table 3) are unusually small.

Discussion

The average P–O distance in $Ca_4(PO_4)_2O$ for 3-coordination of oxygen by Ca ions is 1·538 (10) Å, where the standard deviation (in parentheses) is estimated from the spread of the individual values. The two examples of possible 4-coordination, O(33) and O(34), average 1·537 (18) Å, the same value as for the 3-coordination. The sole example of 2-coordination is O(24), with P(2)–O(24) = 1·511 Å, which is appropriately less than the P–O distances for 3-coordinated oxygens.

The average P–O distances in the P(1), P(2), P(3) and P(4) PO_4 groups are 1·533 (5), 1·537 (19), 1·535 (14) and 1·541 (8) Å respectively. The standard deviations (in parentheses) were estimated from the spread of the individual values. The average for all PO_4 groups is 1·537 Å, with a standard deviation of 0·012 Å when the spread of the individual values is considered. This agrees very well with the average value of 1·539 Å obtained by Baur & Khan (1970) by averaging over PO_4 groups in various forms, *i.e.* $H_2PO_4^-$ *etc.*, in several structures found in the literature.

In the usual considerations of coordination polyhedra, attention is given to the configuration within a covalently bonded group or to the arrangement of oxygen atoms around a central cation. In the case of the $O(Ca)_4$ groupings in the $Ca_4(PO_4)_2O$ structure, one must instead consider the arrangement of cations around an oxygen atom. The $Ca\cdots O^{2-}$ distance is unusually small. The $Ca\cdots O^{2-}$ distance in CaO, which has the NaCl structure, is 2·406 Å (Oftedahl, 1927). When this octahedral coordination is scaled down to tetrahedral coordination along the lines suggested by Pauling (1960, pp. 508, 509, 537–538), the resulting $Ca\cdots O^{2-}$ distance is 2·305 Å. The asymmetry of charge around each Ca ion may allow the $Ca\cdots O^{2-}$ distance to decrease further. It is noteworthy that in β-$Ca_3(PO_4)_2$ (Dickens, Schroeder & Brown, in preparation) one Ca in an octahedral site has Ca···O distances of 2·238 (4) to 2·287 (4) Å to phosphate oxygens.

In the coordination of Ca ions to PO_4 ions in $Ca_4(PO_4)_2O$, (i) each oxygen is usually coordinated to three Ca ions; and (ii) the Ca···O bond tends to be in the plane O–P–O′ where O′ is one of the other three oxygens in the PO_4 group. Thus, the ideal Ca coordination of a PO_4 group appears to be when it shares each of its six edges, making a total PO_4 coordination of six Ca ions. Because Ca bonded to a PO_4 edge forms twice as many bonds to that PO_4 group as does Ca bonded only to a PO_4 apex, the former probably govern the arrangement of Ca ions around the PO_4 group through Ca···Ca repulsions. From the point of view of minimizing Ca···Ca repulsions, face sharing would be preferred. This is more undesirable than edge sharing however, because of increased Ca···P repulsions, as Pauling's third rule states. Therefore, edge sharing where possible appears to be a reasonable compromise. In this case, the three Ca ions and one P atom coordinated to each O atom are arranged in approximately tetrahedral directions about the oxygen atom.

Although the structure of $Ca_4(PO_4)_2O$ is actually monoclinic and acentric ($P2_1$), and the distribution of the quasi-normalized structure factor compares well with that expected for an acentric structure (see above), the positions of the Ca, PO_4 and oxide ions approximately correspond to the requirements of the centric space group $P2_1/m\ 2_1/c\ 2_1/n$, ($Pmcn, D_{2h}^{16}$). All symmetry elements in D_{2h}^{16} except for the 2_1 axis parallel to [010] are pseudo-symmetry elements (designated with primes in the following discussion). These pseudo-symmetry elements are placed in $Ca_4(PO_4)_2O$ as follows.

(i) Mirror planes, *m′*, perpendicular to [100] pass through the P atoms, the Ca(3), Ca(4), Ca(5), and Ca(6) ions and the oxide ions O(1) and O(2).

(ii) A *c′*-glide plane perpendicular to [010] is at $y \sim 0{\cdot}4$ with the present placement of the origin along [010]. (Because $P2_1$ is a polar space group, placement of the origin along [010] is arbitrary in the actual structure.)

(iii) An *n′* glide perpendicular to [001] is at $z = 0{\cdot}5$. Thus, the pseudo-symmetry in the crystal structure is sufficiently pronounced for the existence of a higher-temperature orthorhombic modification to be feasible. Brown & Epstein (1965) noticed appreciable pseudo-orthorhombic symmetry in their X-ray photographs of $Ca_4(PO_4)_2O$ and also concluded that an orthorhombic modification may exist. That the $Ca_4(PO_4)_2O$ structure is capable of absorbing a large amount of energy is revealed by the fact that the melting point of $Ca_4(PO_4)_2O$ is very high (~1710°C, Trömel & Fix, 1961). It is possible that the $Ca_4(PO_4)_2O$ sample studied by Trömel & Zaminer (1959) is an orthorhombic form, stabilized perhaps by some impurity. On the other hand, their sample may have looked orthorhombic because of extensive twinning.

There are eight general positions in space group *Pmcn*. Eight Ca ions [Ca(1), Ca(2) Ca(7), Ca(8) and their counterparts generated by the 2_1 axis of $P2_1$] would be crystallographically equivalent and lie in a general position in *Pmcn*. The remaining atoms under consideration, the equivalent quadruple sets 2[P(1), P(3)], 2[P(2), P(4)], 2[Ca(3), Ca(6)], 2[Ca(4), Ca(5)] and 2[O(1), O(2)], would all be in special positions on mirror planes in the orthorhombic structure. Two oxygen atoms of each PO_4 group would lie on the mirror plane, and the remaining two would be related by the mirror plane. The *c*′-glide relationship between $P(1)O_4$ and $P(3)O_4$ groups is such that the equivalency relationships between their oxygen atoms are O(13)$\Leftrightarrow$O(31), O(11)$\Leftrightarrow$O(34), O(12)$\Leftrightarrow$O(32) and O(13)$\Leftrightarrow$O(33). The relationship between $P(2)O_4$ and $P(4)O_4$ is less clear, but it appears (Fig. 1) that a rotation of $P(4)O_4$ by about 90° around *a* (so that it would satisfy the requirements of the mirror plane *m*′) would bring the two PO_4 groups into a *c*-glide relationship. Their oxygen atoms would then be related as follows: O(21)$\Leftrightarrow$O(42), O(24)$\Leftrightarrow$O(43), O(23)$\Leftrightarrow$O(22) and O(41)$\Leftrightarrow$O(44).

The pseudo-symmetry in $Ca_4(PO_4)_2O$ is also of interest because of possible twinning modes. Termier & Richard (1895) state that (001) and (100) (in the present notation) are the lamellar twin planes. This was corroborated by Brown & Epstein (1965), who state that the composition planes for normal twins they observed would be (001) and (100). Twinning in which the (100) and (001) planes are composition planes are the only ones involving pinacoids that could be detected optically. The possible existence of a high-temperature orthorhombic modification with the symmetry elements $2_1/m$ and $2_1/n$ associated with the *a* and *c* axes, respectively, lends strong support for twinning by any of these four pseudo-symmetry operations. Of the remaining symmetry operations, $2_1/c$, which are associated with the *b* axis, only the *c* glide could produce twinning in monoclinic $Ca_4(PO_4)_2O$ because the 2_1 axis is present as a true symmetry element. Twins produced by the *c* glide operation, however, would be 'optical twins' and would not be detected with the polarizing microscope. Note that the plane of the *c* glide lies at the center of the apatite-like layer in $Ca_4(PO_4)_2O$ described below. The existence of a similar layer in $Ca_5(PO_4)_3(OH)$, hydroxyapatite, suggests that the operations corresponding to $2_1/c$ could produce twinning in $Ca_5(PO_4)_3OH$. Although these operations have not been suggested previously for $Ca_5(PO_4)_3OH$, twins of this type [*i.e.* with (100) the twin plane) have been reported (Palache, Berman & Frondel, 1951). One may speculate that a twinning mechanism of this type (which would also produce optical twins) may have some biological significance in that $Ca_5(PO_4)_3OH$ is an idealization of the major inorganic phase in the body. For example, electron micrographs of the apatitic crystals of dental enamel frequently show a plane of demarcation parallel to (100) which could be the composition plane of a twin.

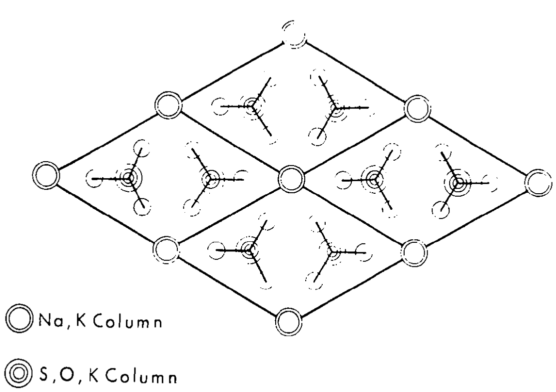

Fig. 4. A schematic drawing of the structure of $K_3Na(SO_4)_2$, glaserite (Gossner, 1928). One S,O,K column in the unit cell points 'up' and the other points 'down'.

Relationship of $Ca_4(PO_4)_2O$ *to other structures*

As was outlined by Dickens & Brown (1972), calcium phosphates typically crystallize in five structural types: (i) structures related to $Ca_5(PO_4)_3(OH,F)$, hydroxyapatite, (ii) structures containing $CaPO_4$ chains and sheets, (iii) structures related to $K_3Na(SO_4)_2$, glaserite, (iv) structures related to $Ba_3(PO_4)_2$, and (v) structures related to $MgNH_4PO_4.6H_2O$, struvite.

Only types (i) and (iii) contain both cation–cation and cation–anion columns. The Ca:P ratio of 2:1 in the formula of $Ca_4(PO_4)_2O$ suggests that it may have a structural relationship to glaserite, $K_3Na(SO_4)_2$ (Gossner, 1928). The presence of the oxide ions means, however, that the glaserite-type structure must be modified to accommodate extra, but small, anions. In other structures in which the cation:anion ratio is not 2:1, *e.g.* $Ca_5(PO_4)_2SiO_4$ (Dickens & Brown, 1971*a*) and $Ca_7Mg_9(Ca,Mg)_2(PO_4)_{12}$ (Dickens & Brown, 1971*b*), the semblance of the glaserite structure is retained by resorting to crystallographically systematic cation vacancies in the cation–anion columns. The relationship between the structures of $K_3Na(SO_4)_2$ (glaserite) (Fig. 4) and $Ca_4(PO_4)_2O$ (shown in an *a* projection in Fig. 5) can be seen most readily in Fig. 6. The latter is derived from Fig. 5 by shifting the layer bounded by the broken lines at *A* and *A*′ about 2 Å to the left. (Each layer consists of two sheets of [Ca, Ca] and [Ca, PO_4] columns.) It can be seen that the highly distorted diamond-shaped cells of Fig. 5 have become fairly regular in Fig. 6. Each cell has [Ca, Ca] columns at the corners and two [Ca, PO_4] columns on the major diagonal, much as they are in Fig. 4. The unit cell of $Ca_4(PO_4)_2O$ corresponds to four glaserite cells.

With the idealization of the structure of $Ca_4(PO_4)_2O$, it is now possible to see why the layers in $Ca_4(PO_4)_2O$ are shifted. In the structure shown in Fig. 6, O(2) would have coordinated to only three calcium atoms, Ca(7), Ca(8) and Ca(5) at three apexes of a tetrahedron; Ca(4) is too far away along *a* to coordinate to O(2). Similarly, O(1) would coordinate to Ca(1), Ca(2) and Ca(4) but not to Ca(5). When the layer *A–A'* shifts to its actual position, as shown in Fig. 5, Ca(3) comes into coordination with O(2) and Ca(6) with O(1) so that each oxygen can have full tetrahedral coordination.

The idealized structure approximates orthohexagonal symmetry, suggesting that the orthorhombic, high-temperature form postulated above may be orthohexagonal if O(1) and O(2) become mobile at higher temperatures.

The lanthanide elements form compounds of the type M_2SiO_4O, which for purposes of comparison with $Ca_4(PO_4)_2O$ may be written $M_4(SiO_4)_2O_2$. The lanthanide oxysilicates actually form two structurally different series with the demarcation occurring at Tb (Felsche, 1971). In both series of compounds (Smolin & Tkachev, 1969; Smolin, 1970), there are sheets each of which contains two cation–anion columns for every one cation–cation column, and the oxide ions have tetrahedral coordination of cations as they do in $Ca_4(PO_4)_2O$, but the juxtapositions of these sheets differ significantly from those in $Ca_4(PO_4)_2O$ and glaserite. Thus, there is only a somewhat tenuous relationship between the structures of $Ca_4(PO_4)_2O$ and the lanthanide oxysilicates.

The $Ca_4(PO_4)_2O$ structure also bears a surprising resemblance to part of the $Ca_5(PO_4)_3OH$ structure (Kay, Young & Posner, 1964), *i.e.* to structural type (i) described above.

The atoms inside the *BB'* layer in Fig. 7, which depicts six unit cells of $Ca_5(PO_4)_3OH$, are compared in

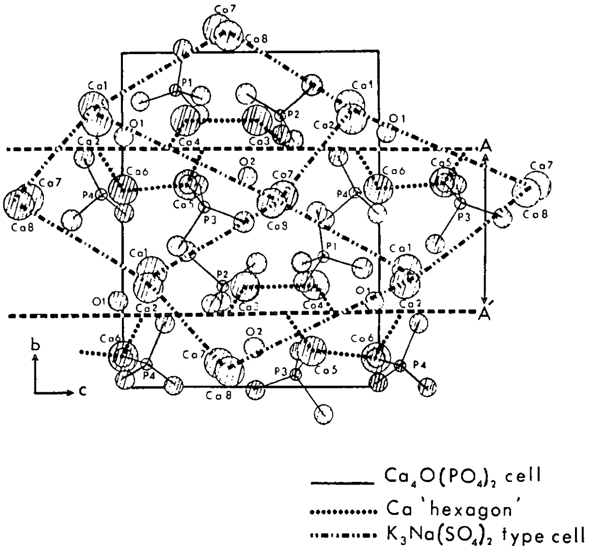

Fig. 5. The relationship of $Ca_4(PO_4)_2O$ to $K_3Na(SO_4)_2$ (glaserite) and $Ca_5(PO_4)_3OH$ (hydroxyapatite). The glaserite-type pseudo-cell in $Ca_4(PO_4)_2O$ is shown by -·-·- lines. The actual cell of $Ca_4(PO_4)_2O$ is shown by solid lines. The layer *AA'* is the 'apatitic' layer in $Ca_4(PO_4)_2O$ and encompasses two sheets of [Ca, Ca] and [Ca, PO_4] columns (see text). The dotted lines show the vestiges in $Ca_4(PO_4)_2O$ of the Ca 'hexagons' in $Ca_5(PO_4)_3OH$.

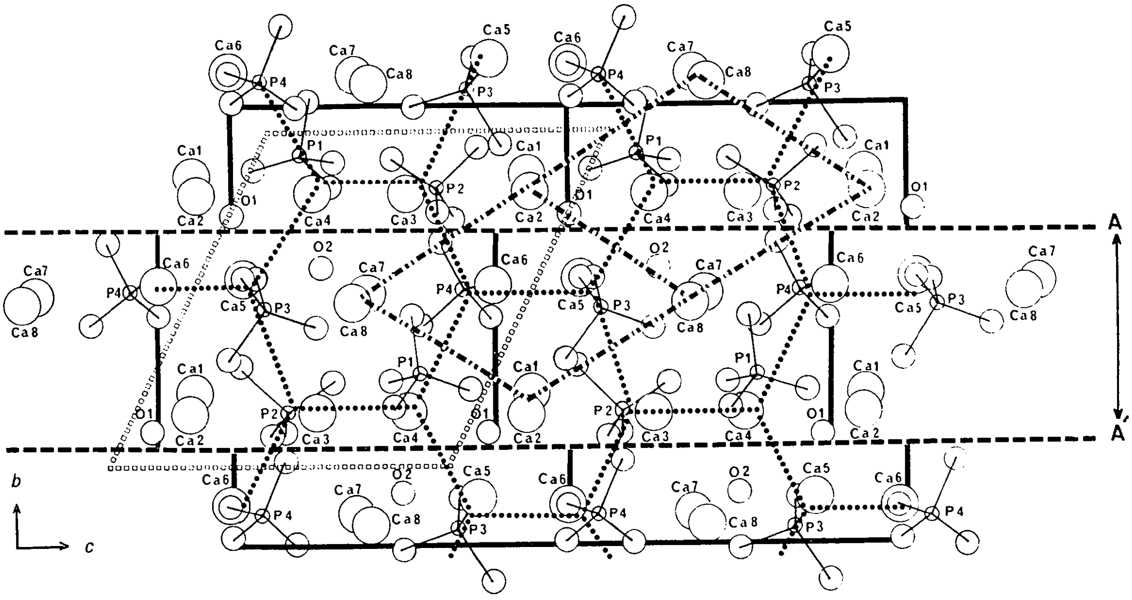

Fig. 6. An idealization of the $Ca_4(PO_4)_2O$ structure. The diagram in Fig. 5 has been cut along the lines *A* and *A'*, and the *AA'* layer moved to the left by ~2 Å. In this idealization the structure is hexagonal if the oxide ions O(1) and O(2) are either ignored or placed on the nearest [Ca, Ca] column. The $K_3Na(SO_4)_2$-type cell is represented by -·-·-. A hexagonal-type cell is shown by dotted lines. A $Ca_5(PO_4)_3OH$-type cell is shown by lines of open squares.

Fig. 8 with atoms in the 'apatitic layer' *AA'* of Fig. 5. Although there are some significant differences in orientation of PO_4 groups, both structures contain similarly positioned [Ca,Ca] and [Ca,PO_4] columns comprising two sheets in each layer. Thus, in the relationship of these 'apatite layers' in $Ca_4(PO_4)_2O$ and $Ca_5(PO_4)_3OH$, the cation–cation columns [Ca(1), Ca(2)] and [Ca(7), Ca(8)] in $Ca_4(PO_4)_2O$ correspond to the calcium columns Ca(I) in $Ca_5(PO_4)_3OH$. Each of the pairs [Ca(3), Ca(4)] and [Ca(5), Ca(6)] in $Ca_4(PO_4)_2O$ corresponds to one side of a Ca(II) 'hexagon' in $Ca_5(PO_4)_3OH$. In this relationship, the locations of the oxide ions O(1) and O(2) in $Ca_4(PO_4)_2O$ correspond to the locations of the OH ions in $Ca_5(PO_4)_3OH$. Because they are actually located in the neighboring apatitic layer in the complete $Ca_4(PO_4)_2O$ structure whereas the OH ions are not in an apatitic layer in $Ca_5(PO_4)_3OH$ the oxide ions account for much of the misorientation of the PO_4 groups in $Ca_4(PO_4)_2O$ as compared with $Ca_5(PO_4)_3OH$.

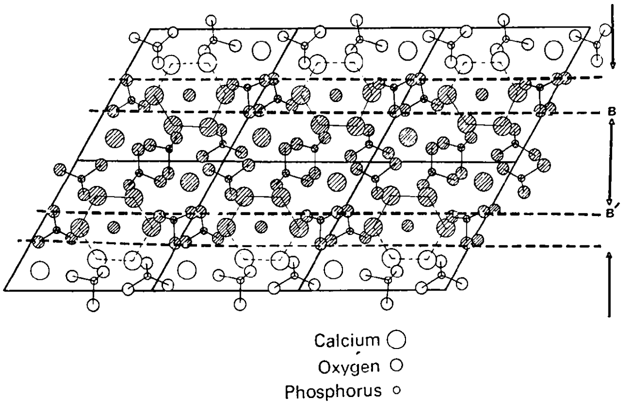

Fig. 7. The structure of $Ca_5(PO_4)_3OH$ (Kay, Young & Posner, 1964). The OH site may be seen in the center of the Ca hexagon in the center of each unit cell. The shaded region is common to the structures of $Ca_5(PO_4)_3OH$ and $Ca_8H_2(PO_4)_6.5H_2O$ Brown, 1962). The layer *BB'* is common to the structures of $Ca_5(PO_4)_3OH$ and $Ca_4(PO_4)_2O$.

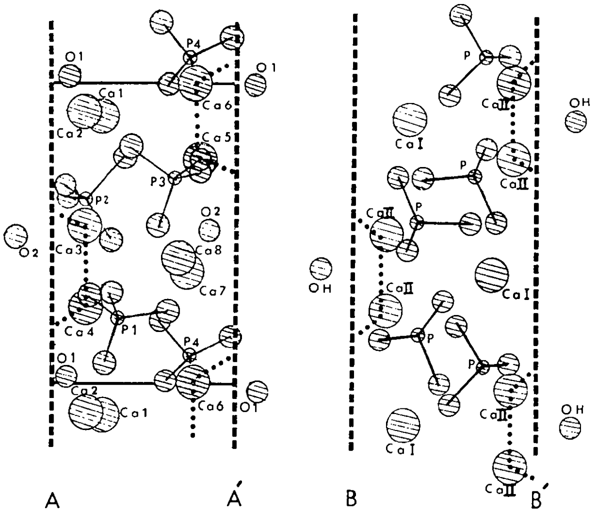

Fig. 8. A comparison of the apatitic layers in $Ca_4(PO_4)_2O$ (*AA'*) and $Ca_5(PO_4)_3OH$ (*BB'*).

The salt $Ca_8H_2(PO_4)_6.5H_2O$ is also known to contain an apatitic layer (Brown, 1962, 1966). In that case, however, the layer is thicker than the one in $Ca_4(PO_4)_2O$ (approximating the shaded area in Fig. 7) and the atomic positions are closer to those of $Ca_5(PO_4)_3OH$.

A more complete relationship between $Ca_4(PO_4)_2O$ and $Ca_5(PO_4)_3OH$ can be derived from the idealized glaserite structures given in Fig. 4 and Fig. 6. If all [Ca(7), Ca(8)] columns in the next layer below (towards the bottom of Fig. 6) are replaced by [OH,OH] columns and the oxide ions O(1) and O(2) are removed, one obtains the approximation for the $Ca_5(PO_4)_3OH$ structure first derived from glaserite by Wondratschek (1963). The unit cell for $Ca_5(PO_4)_3OH$, defined by lines of open squares in Fig. 6, is hexagonal and in this projection consists of three glaserite unit cells. Since, as noted above, the $Ca_4(PO_4)_2O$ unit cell contains four glaserite units, the $Ca_4(PO_4)_2O/Ca_5(PO_4)_3OH$ unit-cell relationship is $\frac{4}{3}$, in contrast with the ratio of the volumes of the two cells which is very close to $\frac{3}{2}$. The difference is consistent with the fact that each glaserite-like unit cell contains $[Ca_4(PO_4)_2O]$ in $Ca_4(PO_4)_2O$ and only $[Ca_{3\cdot33}(PO_4)_2(OH)_{0\cdot67}]$ on the average in $Ca_5(PO_4)_3OH$.

The coordination of the Ca(II) ion in $Ca_5(PO_4)_3OH$ is to nine oxygens comprising three PO_4 apexes and three PO_4 edges. In $Ca_4(PO_4)_2O$ the coordinations of the corresponding Ca(1), Ca(2), Ca(7), Ca(8) ions are all seven, including at the most [for Ca(2) and Ca(7)] two PO_4 edges. Each of these cations is also coordinated to an oxide ion. Sevenfold coordination of Ca in calcium phosphates is far more common than ninefold, the only clear example of which in calcium phosphates is the Ca ion on the threefold axis in $Ca_5(PO_4)_3OH$. Note that the ninefold coordination of Ca in the aragonite phase of $CaCO_3$ is a consequence of (i) the overall packing giving a higher density for aragonite (the high-pressure phase) over that of calcite, and (ii) the smaller O···O separation in the edge of the Co_3 group compared to that in the PO_4 group allowing more oxygens to enter a given size of coordination polyhedron. Since apatites are among the most stable calcium phosphates, the ninefold coordination of Ca(II) in $Ca_5(PO_4)_3OH$ may be a concomitant of efficient packing of the other ions. This may account for the observation that Ca is on the borderline of apatite stability in terms of its radius.

The sequence Ca(II)···O(3)–P–O(3')···Ca(II) in $Ca_5(PO_4)_3OH$ is reproduced quite well in $Ca_4(PO_4)_2O$ in the sequences Ca(3)···O(22)–P(2)–O(23)···Ca(3); Ca(4)···O(12)–P(1)–O(13)···Ca(4); Ca(5)···O(33)–P(3)–O(32)···Ca(5); Ca(6)···O(41)–P(4)–O(44)···Ca(6). The O···Ca···O columns involving Ca(4), Ca(5) and Ca(6) are fairly straight, but the one involving Ca(3) and the oxygens of the P(2)O_4 group is more distorted than the others.

Epitaxy, the ordered growth of one substance on another, is often thought of as being governed chiefly by the metric fits of networks based on the unit cell translations. While epitaxy is certainly not rare, especially if the conditions under which the second phase is forced to grow on the first are sufficiently drastic, in practice only a few orientations are found. Under the mild conditions found *in vivo*, good chemical fits are obviously required. The combination of good metric and chemical fits between $Ca_5(PO_4)_3OH$ and $Ca_8H_2(PO_4)_6.5H_2O$ makes epitaxy between these two compounds very important (Brown, Smith, Lehr & Frazier, 1962; Brown, 1966). The unit cells of $Ca_5(PO_4)_3OH$ and $Ca_4(PO_4)_2O$ (Table 4) suggest that there will be many good metric fits of networks between these two compounds. Because of the structural similarities between $Ca_5(PO_4)_3OH$ and $Ca_4(PO_4)_2O$, epitaxy between them may have considerable importance. Undetected epitaxy between $Ca_5(PO_4)_3OH$ and $Ca_4(PO_4)_2O$ would increase the Ca:P ratio of an apparent apatite above 1·667 and on a fine scale would resemble solid solution. It would also result in an increase in the apparent c unit-cell dimension and probably a reduction in the apparent a dimension relative to the values for pure $Ca_5(PO_4)_3OH$, [because $\frac{3}{2}(d_{100})$ of $Ca_5(PO_4)_3OH$ is less than b of $Ca_4(PO_4)_2O$, while the two a dimensions are approximately equal]. $Ca_5(PO_4)_3OH$ is therefore an unusual salt in that it has two related salts with which it may enter into epitaxic relationships. One salt, $Ca_8H_2(PO_4)_6.5H_2O$, is more acidic, and the other, $Ca_4(PO_4)_2O$, is more basic.

Table 4. *A comparison of the unit cells of* $Ca_5(PO_4)_3OH$(I) *and* $Ca_4(PO_4)_2O$(II)

	I	II
a	9·432 Å	9·462 Å
b	9·432	11·965
c	6·881	7·023
γ	120°	90·8°
Volume	530 Å^3	795 Å^3
Space group	$P6_3/m$	$P2_1$

$d_{100}(I) \times 1·5 = 12·27$ Å
530 Å^3 × 1·5 = 795 Å^3

Although production of $Ca_4(PO_4)_2O$ itself in an aqueous environment would be difficult because of the oxide ion, a carbonate-containing product may form more easily. $Ca_4(PO_4)_2O$ is known to react with CO_2 at elevated temperatures, although the reaction products have not yet been identified. Epitaxy between carbonation products of $Ca_4(PO_4)_2O$ and apatites may be important in the problem of carbonate apatites.

J. S. Bowen and P. B. Kingsbury provided technical help. This investigation was supported in part by research grant DE-00572 to the American Dental Association and by contract to the National Bureau of standards from the National Institute of Dental Research. Much of the computer time was obtained through the facilities of the Computer Science Center, University of Maryland, College Park, Maryland 20742.

References

Alexander, L. E. & Smith, G. (1962). *Acta Cryst.* **15**, 983–1004.

Alexander, L. E. & Smith, G. (1964). *Acta Cryst.* **17**, 1195–1201.

Baur, W. H. & Khan, A. A. (1970). *Acta Cryst.* **B26**, 1584–1596.

Brown, W. E. (1962). *Nature, Lond.* **196**, 1048–1050.

Brown, W. E. (1966). *Clin. Orthop.* **44**, 205–220.

Brown, W. E. & Epstein, E. F. (1965). *J. Res. Natl. Bur. Stand.* **69**A, 547–551.

Brown, W. E., Smith, J. P., Lehr, J. R. & Frazier, A. W. (1962). *Nature, Lond.* **196**, 1050–1055.

Bücking, H. & Linck, G. (1887). *Stahl Eisen*, **7**, 245–249.

Dickens, B. & Bowen, J. S. (1971). *Acta Cryst.* **B27**, 2247–2255.

Dickens, B., Bowen, J. S. & Brown, W. E. (1971). Abstract G3, American Crystallographic Association Winter Meeting, Columbia, S. C.

Dickens, B. & Brown, W. E. (1971*a*). *Miner. Petrogr. Mitt.* **16**, 1–27.

Dickens, B. & Brown, W. E. (1971*b*). *Miner. Petrogr. Mitt.* **16**, 79–104.

Dickens, B. & Brown, W. E. (1972). *Acta Cryst.* **B28**, 3056–3065

Dickinson, C., Stewart, J. M. & Holden, J. R. (1966). *Acta Cryst.* **21**, 663–670.

Felsche, J. (1971). *Naturwissenschaften*, **58**, 565–566.

Gossner, B. (1928). *Neues Jb. Miner. Geol. Palaeontol.* **57**A, 89–116.

International Tables for X-ray Crystallography (1962). Vol. III, p. 202. Birmingham: Kynoch Press.

Kay, M. I., Young, R. A. & Posner, A. S. (1964). *Nature, Lond.* **204**, 1050–1052.

Larson, A. C. (1970). In *Crystallographic Computing*, edited by F. R. Ahmed. Copenhagen: Munksgaard.

Oftedahl, I. (1927). *Z. Phys. Chem.* **128**, 154–158.

Palache, C., Berman, H. & Frondel, C. (1951). *The System of Mineralogy of J. D. Dana and E. S. Dana*, 7th ed., **2**. New York: John Wiley.

Pauling, L. (1960). *The Nature of the Chemical Bond*, 3rd ed. Ithaca: Cornell Univ. Press.

Reimann, C. W., Mighell, A. D. & Maur, F. A. (1967). *Acta Cryst.* **23**, 135–141.

Smolin, Y. I. (1970). *Sov. Phys. Crystallogr.* **14**, 854–858.

Smolin, Y. I. & Tkachev, S. P. (1969). *Sov. Phys. Crystallogr.* **14**, 14–16.

Stewart, J. M., Kruger, G. J., Ammon, H. L., Dickinson, C. & Hall, S. R. (1972). Technical Report TR-192, The Computer Science Center, Univ. of Maryland, Collegec Park, Maryland 20742.

Termier, M. P. & Richard, M. (1895). *Bull. Soc. Fr. Minér. Crist.* **18**, 391–395.

Trömel, G. & Fix, W. (1961). *Arch. Eisenhüttenwes.* **32**, 209–212.

Trömel, G. & Zaminer, C. (1959). *Arch. Eisenhüttenwes.* **30**, 205–209.

Wondratschek, H. (1963). *Neues Jb. Mineral. Abhandl.* **99**, 113–160.

Zachariasen, W. H. (1963). *Acta Cryst.* **16**, 1139–1144.

Zachariasen, W. H. (1967). *Acta Cryst.* **23**, 558–564.